UNIVERSIDADE DE SÃO PAULO

INSTITUTO DE FÍSICA
CAIXA POSTAL 66318
05315-970 SÃO PAULO - SP
BRASIL

PUBLICAÇÕES

IFUSP/P-1260

DIFFRACTIVE MASS SPECTRA AT HERA IN THE INTERACTING GLUON MODEL

F.O. Durães, F.S. Navarra
Instituto de Física, Universidade de São Paulo

G. Wilk
Instituto de Física, Universidade de São Paulo and
Soltan Institute for Nuclear Studies, Nuclear Theory Department
ul. Hoża 69, 00-681 Warsaw, Poland

Março/1997

Pág. 1 - 10

Diffractive Mass Spectra at HERA in the Interacting Gluon Model

F.O. Durães[1]*, F.S. Navarra[1]† and G. Wilk[1,2]‡
[1]*Instituto de Física, Universidade de São Paulo*
C.P. 66318, 05389-970 São Paulo, SP, Brazil
[2]*Soltan Institute for Nuclear Studies, Nuclear Theory Department*
ul. Hoża 69, 00-681 Warsaw, Poland

March 13, 1997

Abstract

We have successfully applied the Interacting Gluon Model (IGM) to calculate diffractive mass spectra measured recently in e-p collisions at HERA. We show that it is possible to treat them in terms of gluon-gluon collisions in the same way as was done before for hadronic collisions. Analysis of available data is performed.

PACS number(s): 13.85.Qk, 11.55.Jy

1 Introduction

In the last years, diffractive scattering processes have received increasing attention for several reasons. They are, among other things, related to the large rapidity gap physics usually interpreted in terms of Pomeron exchange [1]. In hadronic diffractive scattering, one of the incoming hadrons emerges from the collision only slightly deflected and there is a large rapidity gap between it and the other final state particles resulting from the other excited hadron. In the standard Regge theory diffraction is visualised as due to the Pomeron exchange which implies that the excited mass spectrum behaves like $1/M_X^2$ and does

*e-mail: dunga@uspif.if.usp.br
†e-mail: navarra@uspif.if.usp.br
‡e-mail: wilk@fuw.edu.pl

not depend on the energy [2]. The exact nature of the Pomeron in QCD is, however, not yet elucidated. The same phenomena can therefore be understood without mentioning the name of Pomeron altogether by treating $I\!P$ as a *preformed colour singlet* object consisting of only a part of the gluonic content of the diffractive projectile which is then absorbed by the other hadron [3]. One possible realization of this idea was developed recently by us [4] (for earlier similar attempts see [5]).

The first test of a theory (or a model) of diffractive dissociation (DD) is the ability to properly describe the mass (M_X) distribution of diffracted systems, which has been measured in many hadronic collision experiments [6] and parametrized as $(M_X^2)^{-\alpha}$ with $\alpha \simeq 1$.

Very recently diffractive mass spectra have been measured also in photoproduction processes at high energies at HERA [7]. They were interpreted there in terms of standard Regge theory. In this work we would like to analyse these data using instead the Interacting Gluon Model (IGM) in the way proposed in [4]. The advantage of such approach is the possibility to check what part of the results is due to the simple implementation of conservation laws (notice that IGM was designed in such a way that the energy-momentum conservation is taken care of before all other dynamical aspects - a feature very appropriate for the study of all kinds of energy flows). It means that all notions to the Pomeron (or $I\!P$) in what follows is just symbolic representation of the DD process.

2 IGM picture of a diffractive event

As mentioned in [7], at the HERA electron-proton collider the bulk of the cross section corresponds to photoproduction, in which a beam electron is scattered through a very small angle and a quasi-real photon interacts with the proton. For such small virtualities the dominant interaction mechanism takes place via fluctuation of the photon into a hadronic state which interacts with the proton via the strong force. High energy photoproduction therefore exhibits similar characteristics to hadron-hadron interactions.

In Fig. 1 we show schematically the IGM picture of a diffractive event in photon-proton collision. According to it, during the interaction the photon is converted into a hadronic (mesonic) state and then interacts with the incoming proton [8]. The meson-proton interaction follows then the usual IGM picture, namely: the valence quarks fly through essentially undisturbed whereas the gluonic clouds of both projectiles interact strongly with each other (by gluonic clouds we understand a sort of "effective gluons" which include also their fluctuations seen as $\bar{q}q$ sea pairs). The meson looses fraction x of its original momentum and gets excited forming what we call a *leading jet* (LJ) carrying $x_L = 1 - x$ fraction of the initial momentum. The proton, which we shall call here the diffracted proton, looses only a fraction y of its momentum but otherwise remains intact [9].

In the limit $y \to 1$, the whole available energy is stored in M_X which then remains at rest, i.e., $Y_X = 0$. For small values of y we have small masses M_X located at large rapidities Y_X. In order to regard our process as being trully of the DD type we must assume that all gluons from the target proton participating in the collision (i.e., those emitted from the lower vertex in Fig. 1) *have to form a colour singlet.* Only then a large rapidity gap will form separating the diffracted proton (in the lower part of our Fig. 1) and the M_X system (in its upper part), which is the experimental requirement defining a diffractive event. Otherwise a colour string would develop, connecting the diffracted proton and the diffractive cluster, and would eventually decay, filling the rapidity gap with produced secondaries. In this way we are effectively introducing an object resembling closely to what is known as Pomeron ($I\!P$) and therefore in what follows we shall use this notion. The Pomeron may be treated [11] as being composed of partons, i.e., gluons and sea $\bar{q}q$ pairs, in much the same way as hadrons, with some characteristic distribution functions which presumably will become accurately known in HERA experiments [12].

As usual in the IGM [4] we first start with the function $\chi(x,y)$ describing the probability to form a central gluonic fireball (CF) carrying momentum fractions x and y of the two colliding projectiles:

$$\begin{aligned}\chi(x,y) \;&=\; \frac{\chi_0}{2\pi\sqrt{D_{xy}}}\cdot \\ &\cdot \exp\left\{-\frac{1}{2D_{xy}}\left[\langle y^2\rangle(x-\langle x\rangle)^2+\langle x^2\rangle(y-\langle y\rangle)^2-2\langle xy\rangle(x-\langle x\rangle)(y-\langle y\rangle)\right]\right\}. \qquad (1)\end{aligned}$$

For our specific needs in this paper (application to DD events) where we are mostly interested in the x and M_X^2 behaviour of the results, it is usefull to present (1) in the form where the x-dependence is factorized out:

$$\chi(x,y)=\frac{\chi_0}{2\pi\sqrt{D_{xy}}}\cdot\exp\left[-\frac{(y-\langle y\rangle)^2}{2\langle y^2\rangle}\right]\cdot\exp\left\{-\frac{\langle y^2\rangle}{2D_{xy}}\left[x-\langle x\rangle-\frac{\langle xy\rangle}{\langle y^2\rangle}(y-\langle y\rangle)\right]^2\right\}. \qquad (2)$$

In the above equations

$$D_{xy} \;=\; \langle x^2\rangle\langle y^2\rangle-\langle xy\rangle^2 \qquad (3)$$

and

$$\langle x^n y^m\rangle \;=\; \int_0^1 dx\, x^n\int_0^{y_{max}} dy\, y^m\,\omega(x,y). \qquad (4)$$

Here χ_0 denotes the normalization factor provided by the requirement that $\int_0^1 dx\int_0^1 dy\,\chi(x,y)\theta(xy-K^2_{min})=1$ with $K_{min}=\frac{m_0}{\sqrt{s}}$ being the minimal inelasticity defined by the mass m_0 of the lightest possible CF. In the above expression $y_{max}=\frac{M_X^2}{s}$. This upper cut-off, not present in the non-diffractive formulation of the IGM (where $y_{max}=1$), is necessary to adapt the standard IGM to DD collisions. It is a kinematical restriction preventing the gluons coming from the diffracted proton (and forming our object $I\!P$) to carry more energy than what is released in the diffractive system. Nevertheless, as will be seen below, it plays a central role in the adaptation of the IGM to DD processes being responsable for its proper M_X^2 dependence. The, so called, spectral function $\omega(x,y)$ contains all the dynamical inputs of the IGM in the general form given by (cf. [10])

$$\omega(x,y) \;=\; \frac{\sigma_{gg}(xys)}{\sigma(s)}\,G(x)\,G(y)\,\Theta\left(xy-K^2_{min}\right), \qquad (5)$$

where G's denote the effective number of gluons from the corresponding projectiles (approximated by the respective gluonic structure functions) and σ_{gg} and σ are the gluonic and hadronic cross sections, respectively.

The moments $\langle q^n\rangle$, $q=x,y$ (we only require $n=1,2$) are given by (4) and are the only places where dynamical quantities like the gluonic and hadronic cross sections appear in the IGM. At this point we

emphasize that we are all the time dealing with a meson (essentially the ρ^0)-proton scattering. However, as was said above, we are in fact selecting a special class of events and therefore we must choose the correct dynamical inputs in the present situation, specially the gluon distribution inside the diffracted proton and the hadronic cross section σ appearing in ω. As a first approximation we shall take $G^{\rm P}(y)=G^p(y)=G(y)$ (cf. [11]), with $G(y)=p(m+1)\frac{(1-y)^m}{y}$, with m=5, the same expression already used by us before [10]. Here, for simplicity, we assume the vector meson to be ρ^0 and take $G^{\rho^0}(x)=G^{\pi}(x)$. The fraction of diffracted nucleon momentum, p, allocated specifically to the $I\!P$ gluonic cluster and the hadronic cross section σ are both unknown. However, they always appear in ω as a ratio $(\frac{p}{\sigma})$ of parameters and different choices are possible. Just in order to make contact with the present knowledge about the Pomeron, we shall choose

$$\sigma(s) \;=\; \sigma^{\rm Pp}=a+b\ln\frac{s}{s_0} \qquad (6)$$

where $s_0=1\ GeV^2$ and $a=2.6$mb and $b=0.01$mb are parameters fixed from a previous [4] systematic data analysis. As it can be seen, $\sigma(s)$ turns out to be a very slowly varying function of $\sqrt{s}$ assuming values between 2.6 and 3.0 mb, which is a well accepted value for the Pomeron-proton cross section, and $p\simeq 0.05$ (cf. [4]). Since the parameter $\frac{p}{\sigma}$ has been fixed considering the proton-proton diffractive dissociation and we are now addressing the $p-\rho^0$ case we have some freedom to change σ. In the following we shall also investigate the effect of small changes in the value of m_0 on our final results.

Although in the final numerical calculations the above complete formulation will be used, it is worthwhile to present approximate analytical results in order to illustrate the main characteristic features of the IGM. Keeping only the most singular terms in gluon distribution functions, i.e., $G(x),\simeq\frac{1}{x}$ and only the leading terms in $\sqrt{s}$, one finds that for any choice of σ_{gg} in (5):

(*i*) terms containing $\langle xy\rangle$ can be neglected in comparison to those containing $\langle x^2\rangle$ or $\langle y^2\rangle$;

(*ii*) all moments are related in the following way:

$$\langle x^2\rangle\simeq\frac{1}{2}\langle x\rangle;\qquad \langle y^2\rangle\simeq\frac{1}{2}\langle y\rangle;\qquad \langle y\rangle=y\langle x\rangle, \qquad (7)$$

i.e., all results can be expressed in terms of the $\langle x\rangle$ moment only;

(*iv*) the $\langle x\rangle$ moment has the following simple behaviour depending on the type of σ_{gg} chosen in (5):

$$\langle x\rangle\simeq const,\quad \simeq\ln\left(\frac{sy}{m_0^2}\right),\quad \simeq\frac{1}{2}\ln^2\left(\frac{sy}{m_0^2}\right)\qquad \text{for}\qquad \sigma_{gg}\simeq\frac{m_0^2}{xys},\quad \simeq const,\quad \simeq\ln\left(\frac{xys}{m_0^2}\right), \qquad (8)$$

respectively.

This allows us to write eq.(2) in a very simple form:

$$\chi(x,y)\simeq\frac{\chi_0}{\pi\,y\langle x\rangle}\cdot\exp\left[-\frac{(1-\langle x\rangle)^2}{\langle x\rangle}\right]\cdot\exp\left[-\frac{(x-\langle x\rangle)^2}{\langle x\rangle}\right]. \qquad (9)$$

As already mentioned, the $\frac{1}{y}$ term present in (9) can be traced back to the upper cut-off $y=y_{max}$ in (4) above. Because it is defined by the produced diffractive mass, $y=\frac{M_X^2}{s}$, it provides then automatically the characteristic $\frac{1}{M_X^2}$ behaviour of the diffractive mass spectra as given by eq.(11) below. The other two factors have a much weaker dependence on M_X^2 and they tend to compensate each other (cf. [4]). Notice therefore that already this approximate formula satisfies the main test for the applicability of the model to DD collisions mentioned above, namely it shows the $(M_X^2)^{-\alpha}$ behaviour with $\alpha \simeq 1$.

3 Comparison with experimental data

The IGM diffractive mass spectrum is given by [4]:

$$\begin{aligned} \frac{dN}{dM_X^2} &= \int_0^1 dx \int_0^1 dy\, \chi(x,y)\, \delta\left(M_X^2 - sy\right)\, \Theta\left(xy - K_{min}^2\right) \\ &= \frac{1}{s}\int_{\frac{m_0^2}{M_X^2}}^1 dx\, \chi\left(x, y = \frac{M_X^2}{s}\right), \end{aligned} \tag{10}$$

or, in the approximate form,

$$\frac{dN}{dM_X^2} \simeq \frac{1}{M_X^2}\cdot\frac{\chi_0}{\pi\langle x\rangle}\exp\left[-\frac{(1-\langle x\rangle)^2}{\langle x\rangle}\right]\int_{\frac{m_0^2}{M_X^2}}^1 dx \exp\left[-\frac{(x-\langle x\rangle)^2}{\langle x\rangle}\right]. \tag{11}$$

In Fig. 2 we compare it with the recent data from the H1 collaboration [7]. Figure 2a (2b) presents data for the photon-proton center of mass energy $W = 187$ GeV ($W = 231$GeV). The different curves correspond to the choices I ($m_0 = 0.31$ GeV, $\sigma = 2.7$ mb), II ($m_0 = 0.35$ GeV, $\sigma = 2.7$ mb), III ($m_0 = 0.31$ GeV, $\sigma = 5.4$ mb) and IV ($m_0 = 0.35$ GeV, $\sigma = 5.4$ mb), respectively. As expected, the distribution at low M_X^2 is very sensitive to threshold effects. When we go from the upper to the lower solid (dashed) lines we can observe that the increase of the Pomeron-hadron cross section changes the distribution in such a way that larger masses M_X^2 are favoured.

We would like to stress that in curve II there is no free or new parameter. All parameter values are the same as in our previous paper devoted to hadronic diffraction. It misses only the very small mass region points, where we expect it to be below the data, since we do not include resonance effects. In the large mass region a better agreement with data may be achieved with a somewhat larger value of the Pomeron-hadron cross section. This region may, however, be influenced by other effects, one of which we discuss below.

A very interesting question regarding DD processes is whether or not semihard interactions play a role in diffractive physics. In hadronic non-diffractive collisions semihard collisions are expected to be visible at c.m.s. energies around $\sqrt{s} \simeq 500$ GeV. In such collisions two partons interact with a momentum transfer of $p_T \simeq 2-4$ GeV, forming two so-called minijets. Since $\Lambda_{QCD} \ll p_T \ll \sqrt{s}$, minijet cross sections can be calculated with perturbative QCD and they are large enough to be relevant for minimum bias physics. In the IGM, energy deposition is occuring due to gluon-gluon collisions in both perturbative (semihard) and non-perturbative regimes. The gluon-gluon cross section in eq. (5) is computed with perturbative QCD or with a non-perturbative ansatz according to the scale ($= xys$). The relative importance of minijets with respect to the soft processes was fixed following the experimental estimates of the minijet cross section made by the CERN UA1 and UA5 collaborations in hadronic collisions. We have been assuming so far that the onset of semihard physics in DD occurs at the same energy as in ordinary non-diffractive processes. This may not be true, or even if it is true, there are uncertainties regarding the precise value of the relevant energy scale. In Fig. 3 we repeat the fit of Fig. 2 using only curves II, which are our "conservative" calculation, plotted with solid lines. Since the present energies are not yet very large, we could just neglect the small minijet component. The dashed curves in Fig. 3 show the effect of switching off the semihard contribution. There is only a small enhancement in the tail of the spectra. Without minijets the energy deposition in the central blob of Fig. 1 is decreased and the leading particle, in the upper leg (ρ meson after interaction), is more energetic. It contributes more to the diffractive mass M_X^2 and makes it larger. This effect is negligible for very low M_X^2 but becomes visible at large diffractive masses. Repeating this comparison (total spectrum versus the spectrum without minijets) at higher energies we observe that the magnitude of the minijet contribution is always small and shows always the tendency to produce slightly faster falling distributions at the end of the spectrum. This suggests that in DD processes minijets are unimportant even at very high energies.

4 Summary and conclusions

In conclusion, a straightforward (and with no new parameter) extension of our model of hadronic diffraction to photon-proton reactions is able to fit the data for diffractive mass excitation presented in ref. [7] within small discrepancies. The agreement may become better with some small changes motivated by uncertainties in previous fitting procedures.

The fact that our model is successful means that energy flow in many and different high energy reactions can be understood as an incoherent superposition of parton-parton scatterings constrained by energy conservation and is not very much sensitive to details of the interaction like the exact shape of parton distributions, higher order corrections to partonic cross sections, etc.

Acknowledgements: This work has been supported by FAPESP, CNPQ (Brazil) and KBN (Poland). We would like to warmly thank R. Covolan and E. Ferreira for many fruitful discussions. GW would also like to thank IFUSP for warm hospitality extended to him during his visit there.

References

[1] J.D.Bjorken, *Nucl. Phys. (Proc. Suppl.)* **B25** (1992) 253.

[2] K.Goulianos, *Phys. Rep.* **101** (1983) 169.

[3] A.Edin, G.Ingelman and J.Rathsman, *Phys. Lett.* **B366** (1996) 371 and references therein.

[4] F.O.Durães, F.S.Navarra and G.Wilk, *Phys. Rev.* **D55** (1997) 2708 and references therein.

[5] B.R.Desai and U.P.Sukhatme, *Z. Phys.* **C24** (1984) 277; V.Innocente et al., *Phys. Lett.* **B169** (1986) 285; L.Lönnblad, *Z. Phys.* **C65** (1995) 285; J.C.Collins et al., *Phys. Rev.* **D51** (1995) 3182.

[6] N.A.Amos et al. (E710 Collab.), *Phys. Lett.* **B301** (1993) 313; F.Abe et al. (CDF Collab.), *Phys. Rev.* **D50** (1994) 5535 (and references therein). Cf. also M.Bozzo et al. (UA4 Collab.), *Phys. Lett.* **B136** (1984) 217.

[7] C. Adloff et al., (H1 Collab.), DESY Report DESY 97-009; hep-ex/9702003.

[8] J.Sakurai, *Ann. Phys.* **11** (1960) 1 and *Phys. Rev. Lett.* (1969) 981.

[9] It can be also deflected with some invariant momentum transfer t. However, because the IGM does not include so far any transverse momentum transfers, the results presented here must be regarded as appropriately averaged/integrated over t.

[10] F.O.Durães, F.S.Navarra and G.Wilk, *Phys. Rev.* **D47** (1993) 3049.

[11] G.Ingelman and P.Schlein, *Phys. Lett.* **B152** (1985) 256; A.Donnachie and P.V.Landshoff, *Phys. Lett.* **B191** (1987) 309; *Nucl. Phys.* **B303** (1988) 634.

[12] ZEUS Collaboration: M.Derrick et al., *Z. Phys.* **C68** (1995) 569 and references therein.

Figure Captions

Fig. 1 IGM description of a photon-proton scattering with the formation of a diffractive system of invariant mass M_X.

Fig. 2a Diffractive mass spectrum for γp collisions at $W = 187$ GeV calculted with the IGM (eq.(10)) and compared with H1 data [7]. The different curves correspond to the choices: I ($m_0 = 0.31$ GeV, $\sigma = 2.7$ mb), II ($m_0 = 0.35$ GeV, $\sigma = 2.7$ mb), III ($m_0 = 0.31$ GeV, $\sigma = 5.4$ mb) and IV ($m_0 = 0.35$ GeV, $\sigma = 5.4$ mb), respectively.

Fig. 2b The same as Fig. 2a for $W = 231$ GeV.

Fig. 3a Diffractive mass spectrum for γp collisions at $W = 187$ GeV, curve II of Fig. 2a, shown with a solid line and compared with the same spectrum without the minijet contribution (dashed line).

Fig. 3b The same as Fig. 3a for $W = 231$ GeV.

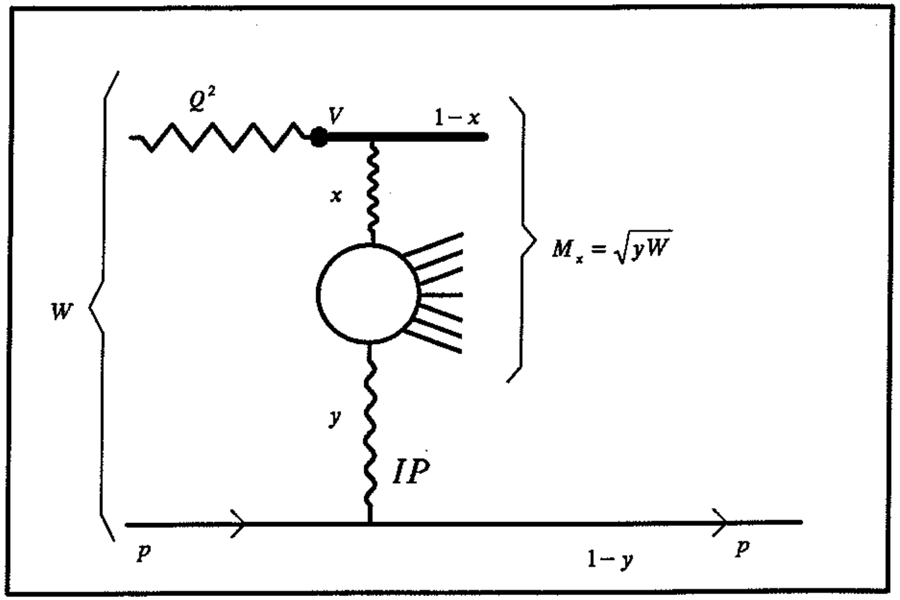

Figure 1

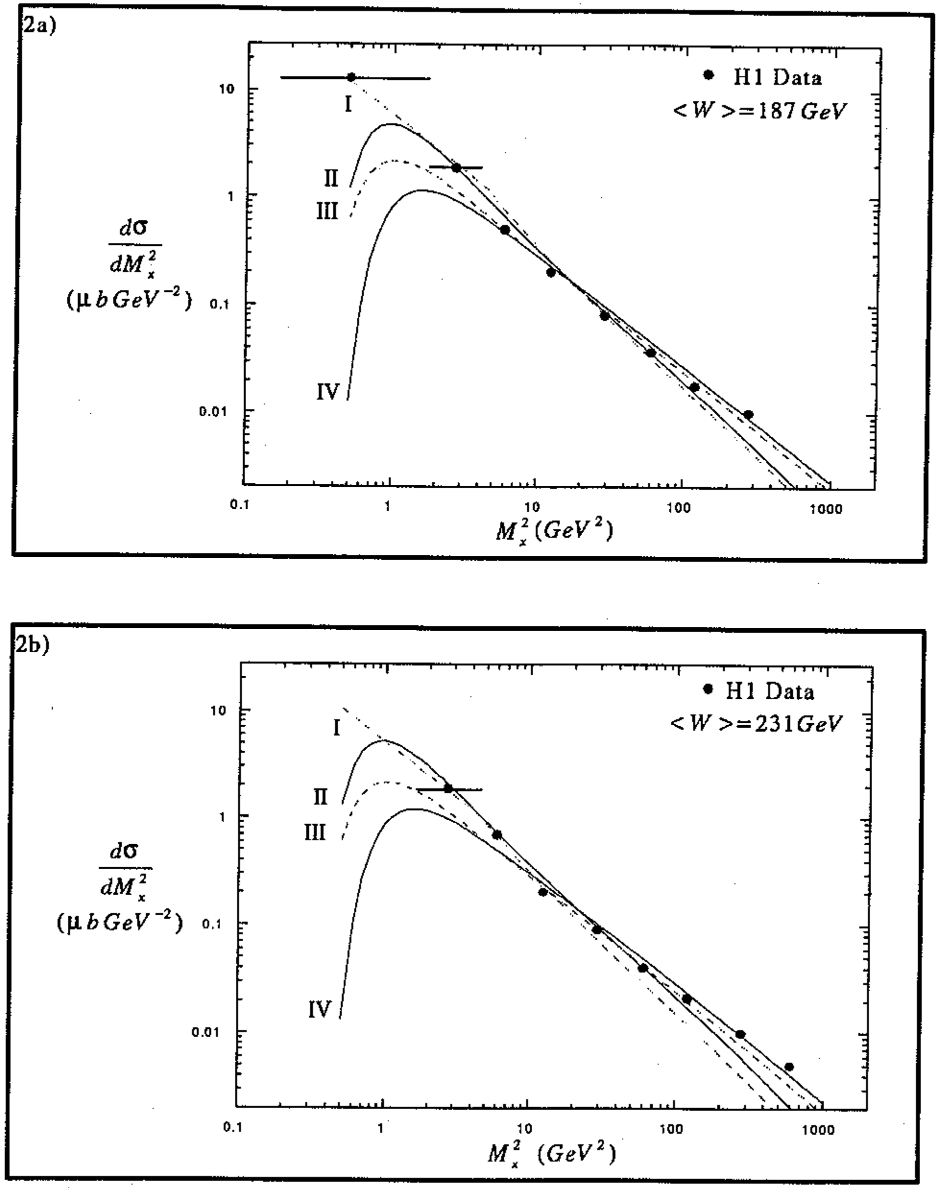

Figure 2

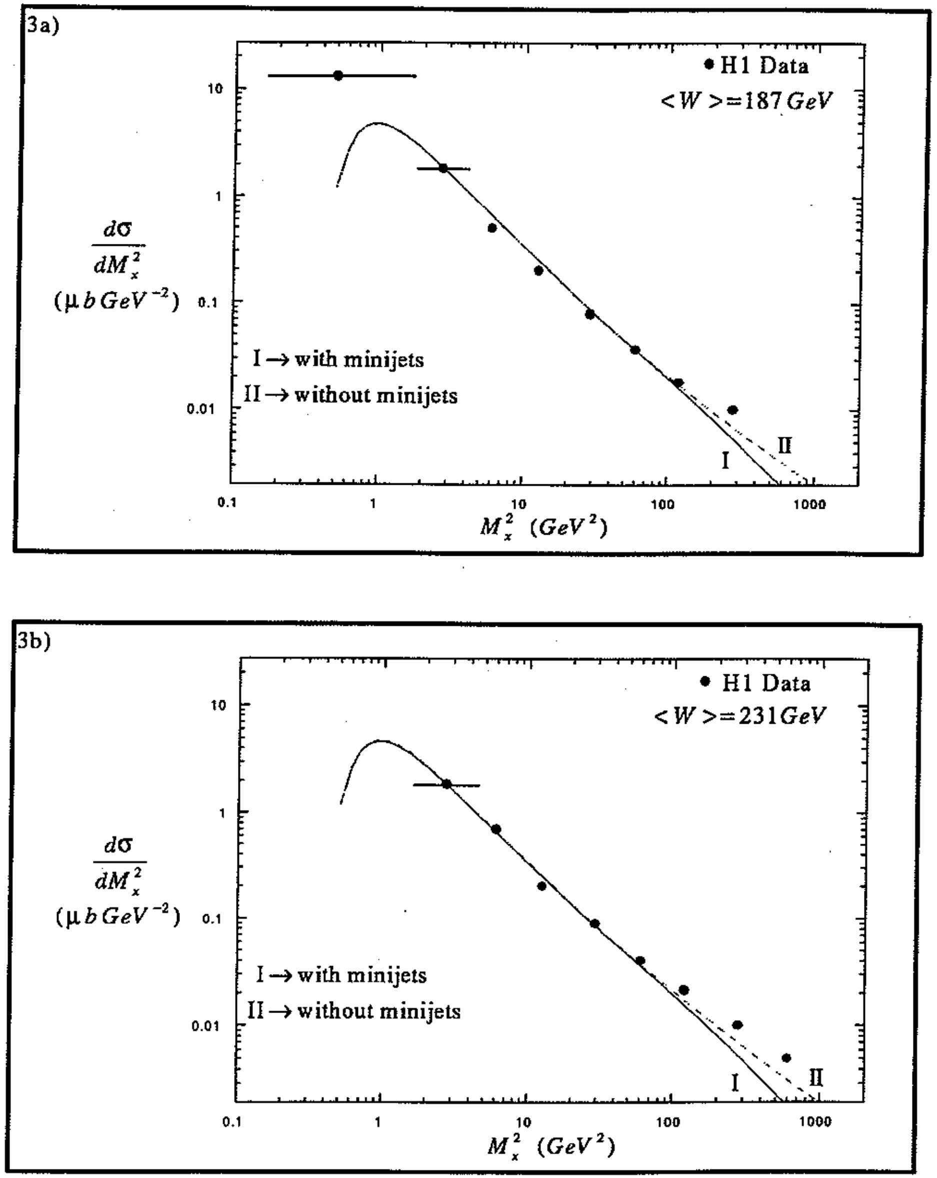

Figure 3